

Beam Coding with Orthogonal Complementary Golay Codes for Signal to Noise Ratio Improvement in Ultrasound Mammography

Y. Kumru, K. Enhos, H. Köyメン

Abstract—In this paper, we report the experimental results on using complementary Golay coded signals at 7.5 MHz to detect breast microcalcifications of 50 μm size. Simulations using complementary Golay coded signals show perfect consistence with the experimental results, confirming the improved signal to noise ratio for complementary Golay coded signals. For improving the success on detecting the microcalcifications, orthogonal complementary Golay sequences having cross-correlation for minimum interference are used as coded signals and compared to tone burst pulse of equal energy in terms of resolution under weak signal conditions. The measurements are conducted using an experimental ultrasound research scanner, Digital Phased Array System (DiPhAS) having 256 channels, a phased array transducer with 7.5 MHz center frequency and the results obtained through experiments are validated by Field-II simulation software. In addition, to investigate the superiority of coded signals in terms of resolution, multipurpose tissue equivalent phantom containing series of monofilament nylon targets, 240 μm in diameter, and cyst-like objects with attenuation of 0.5 dB/[MHz \times cm] is used in the experiments. We obtained ultrasound images of monofilament nylon targets for the evaluation of resolution. Simulation and experimental results show that it is possible to differentiate closely positioned small targets with increased success by using coded excitation in very weak signal conditions.

Keywords—Coded excitation, complementary Golay codes, DiPhAS, medical ultrasound.

I. INTRODUCTION

CODED signals are commonly used in communication, radar and sonar systems due to their advantages and unique properties [1], [2]. In the recent years, using coded signals in medical ultrasound has aroused the interest and a number of studies have been done in this area [21], [22]. Coded excitation has the advantage of achieving images with better quality in medical ultrasound. However, code length limitations, complex circuitry requirements and poor diversity restrict the use of coded signals. Waveform selection is comprehensively studied but the implementation method of the selected waveform is not considered in detail in the literature [18], [23]. The aim of this study is to bridge this gap and achieve an improved detection for the microcalcifications in breast tissue.

Mammography is a diagnostic X-ray imaging technique, widely used to detect microcalcifications which are larger than 50 μm size. Medical ultrasound imaging operating with ultrasonic waves at MHz frequencies is generally preferred as a

follow up test to pursue the progression of pre-diagnosed microcalcifications. Currently, medical ultrasound cannot detect microcalcifications as selectively as mammography. In medical ultrasound imaging, high frequencies would be employed to improve image quality. However, increased frequency results in increased attenuation causing loss of sound intensity and decrease in penetration depth [3].

Even though the most common pulse type used in medical ultrasound imaging is the tone burst pulse due to its simple requirements for the circuitry, the coded signals with unique features are the best nominee for future medical ultrasound imaging systems, which offers significant advantage on the SNR. In this study, orthogonal complementary Golay sequences are used to code the signal. The orthogonal complementary Golay coded excitation is compared to tone burst pulse excitation of equal energy in terms of resolution under weak signal conditions and found favorable, despite the computational overhead involved.

The measurements are conducted using an experimental ultrasound research scanner, DiPhAS having 256 channels, and a phased array transducer with 7.5 MHz center frequency. Moreover, the results obtained through experiments are validated by Field-II simulation software. In addition, to investigate the superiority of coded signals in terms of resolution, the multipurpose tissue equivalent phantom (Nuclear Associates Model 84-317, Fluke Biomedical¹⁾) containing a series of monofilament nylon targets, 240 μm in diameter, with attenuation of 0.5 dB/[MHz \times cm], is used in the experiments. The experiments show that complementary Golay coded signals with 8 chips provide improved range resolution compared to tone burst signal, meanwhile the same SNR is achieved at the output of the matched filter.

This paper is organized as follows. Matched filtering and beamforming concepts are shortly described. Next, the construction of complementary Golay sequences and Pulse Width Modulation (PWM) are provided. Then the simulation results for SNR improvement of complementary Golay coded signals obtained by using Field-II are given. Subsequently, the experimental results achieved by tissue mimicking phantom for sinusoidal burst excitation and complementary Golay coded excitation at center frequency 7.5 MHz are demonstrated. Finally, the conclusion part is provided.

Y. Kumru, K. Enhos, and H. Köyメン are with Bilkent University Acoustic and Underwater Technologies Research Center in Ankara, Turkey (phone: +90 312 290 2457, e-mail: yasin.kumru@bilkent.edu.tr)

II. MATCHED FILTER AND BEAMFORMING CONCEPTS

A. Matched Filtering

Matched filtering is used to maximize the SNR at the receiver output if the received signal is corrupted by Additive White Gaussian Noise (AWGN). The impulse response of a matched filter for a complex valued signal $x(t)$ can be expressed as:

$$h_{MF}(t) = x^*(-t) \quad (1)$$

If a signal is passed through its matched filter, the response of the filter becomes the auto-correlation of the signal. The autocorrelation of the signal is given as:

$$R_x(t) = x(t) * x^*(-t) = \int_{-\infty}^{+\infty} x(\tau)x^*(\tau-t)d\tau \quad (2)$$

The correlation between the transmitted signals and the received signals are investigated in our study by using the matched filter concept. If the received signal is assumed to be the attenuated and shifted version of the transmitted signal and corrupted by AWGN, the received signal (voltage) can be expressed as:

$$y(t) = \alpha x(t - \tau) + N(t) \quad (3)$$

where α is the attenuation constant, τ is the time delay value and $N(t)$ is the AWGN signal. Substituting (3) in (2), an analytical expression of the matched filter output can be expressed as:

$$R_{xy}(t) = y(t) * h_{MF}(t) \quad (4)$$

$$R_{xy}(t) = \int_{-\infty}^{+\infty} [A x(m - \tau) + N(m)] x^*(m - t) dm \quad (5)$$

Applying change of variables which is $n = m - t$ on (5) gives:

$$R_{xy}(t) = \int_{-\infty}^{+\infty} [A x(n + t - \tau) + N(n + t)] x^*(n) dn \quad (6)$$

Note that (6) is also the expression for the expectation of $x(t)$ and $y(t + n)$, $E[x(t)y(t + n)]$, which is the crosscorrelation of the received signal and the transmitted signal [2], [4].

B. Spatial Filtering: Correlation Based Beamforming

Beamforming enhances the performance of an ultrasound array in terms of detectability, resolution and directional measurement of received echoes [1], [5]-[8], [20]. The most common and well-known beamforming technique is Delay and Sum (DAS) beamforming in which the time delay and an amplitude weight for each element in the array are applied on the received echoes in such a way that particular signals experience constructive interference while other signals experience destructive interference. In other words, the received echoes are synchronized according to the delays, weighted and then summed in time domain to maximize the array sensitivity to a particular position. Since delaying, weighting, summing and correlation are all linear processes, the

correlation-based beamforming technique is employed in this study instead of DAS beamforming. The correlation based beamformer consists of taking correlation between the stored data at each channel and the reference signal, applying a sample delay μ and then summing the resulting signals, as displayed in Fig. 1.

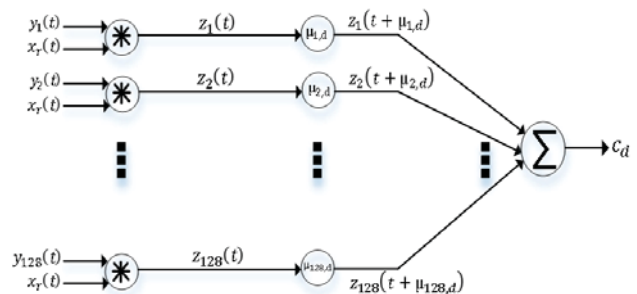


Fig. 1 Block Diagram of a Correlation Based Beamformer

The notation used in Fig. 1 is as follows: $y_i(t)$ represents the received data at i th element, $x_r(t)$ is the reference signal, $z_i(t)$ is the correlation result of the received data at i th element, $\mu_{i,d}$ is the sample delay for i th element and depth d and $c_d(t)$ is the beamformer output corresponding to a depth d .

III. COMPLEMENTARY GOLAY SEQUENCES

A. Construction of Complementary Golay Sequences

Complementary Golay codes are the most well-known complementary codes. They have aroused more interest in comparison with other codes proposed in medical ultrasonography.

If the summation of aperiodic autocorrelations of each sequence in a set is zero for every non-zero phase shift, the set is called complementary set [9]-[13]. The set of two complementary Golay sequences, $a = (a_0 a_1 \dots a_{n-1})$ and $b = (b_0 b_1 \dots b_{n-1})$ with length n , form the complementary Golay pairs. The aperiodic autocorrelation can be expressed as:

$$ACF_{a,j} = \sum_{i=0}^{i=n-j} a_i a_{i+j} \quad \text{and} \quad ACF_{b,j} = \sum_{i=0}^{i=n-j} b_i b_{i+j} \quad (7)$$

Then, summation of aperiodic autocorrelations can be written according to the complementarity condition of Golay sequences,

$$\begin{aligned} ACF_{a,j} + ACF_{b,j} &= 0 \quad \text{for } j \neq 0 \\ ACF_{a,j} + ACF_{b,j} &= 2n \quad \text{for } j = 0 \end{aligned} \quad (8)$$

Complementary Golay sequences are also known as bipolar sequences since a_i 's and b_i 's take the values of +1's and -1's. In the experiments, two complementary Golay sequences of length 8 chips with 2 cycles per chip are used as shown in Fig. 2. These two sequences form a Golay Pair (GP) which is represented as GP (A,B). These sequences are generated according to the Binary Phase Shift Keying (BPSK) modulation scheme in which 180° phase shift exists between bit "1" and bit "-1".

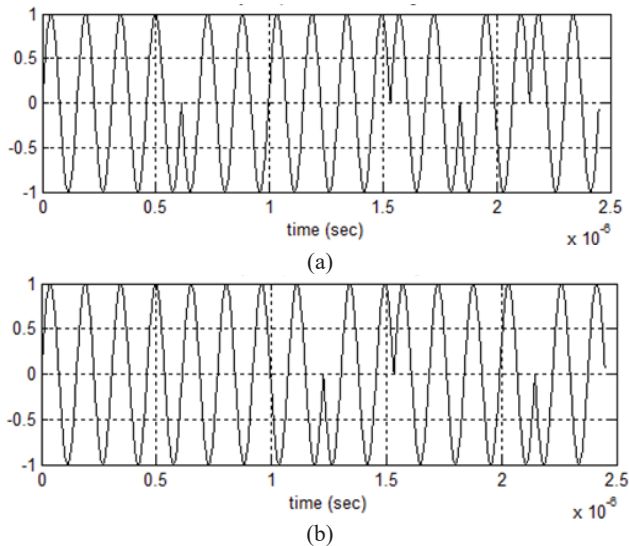


Fig. 2 (a) Golay Sequence A with length 8 which is represented as "11000101", (b) Golay Sequence B with length 8 which is represented as "11110110"

Using (7) and (8), it can be shown that complementary Golay sequences shown in Fig. 2 satisfy the complementarity condition which is illustrated in Fig 3.

B. Generating Excitation Signals by PWM

DiPhAS supports transmit waveforms which can be generated by PWM. PWM is a modulation technique used for

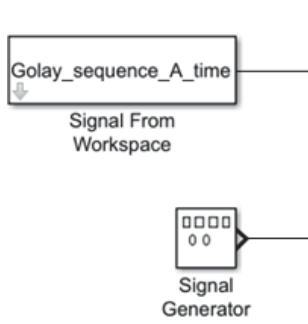


Fig. 4 MATLAB Simulink model with three level PWM Generator

IV. SIMULATION RESULTS

A. SNR Improvement

SNR improvement as a function of depth for the complementary Golay coded signal compared to sinusoidal burst signal at 4 MHz is presented in this section. All simulations in this study are performed with a simulation software, Field II. A concave and round transducer consisting of small elements with a focal point at 2 cm is used in the simulations. The geometry of the transducer is illustrated in Fig.

encoding a message signal into a pulsing signal. In this study, the complementary Golay coded signals and sinusoidal burst signal with equal energy are converted into a PWM signal to be transmitted from ultrasound probe. MATLAB Simulink is used for the PWM generation process and the model used in Simulink to generate PWM signal is shown in Fig. 4.

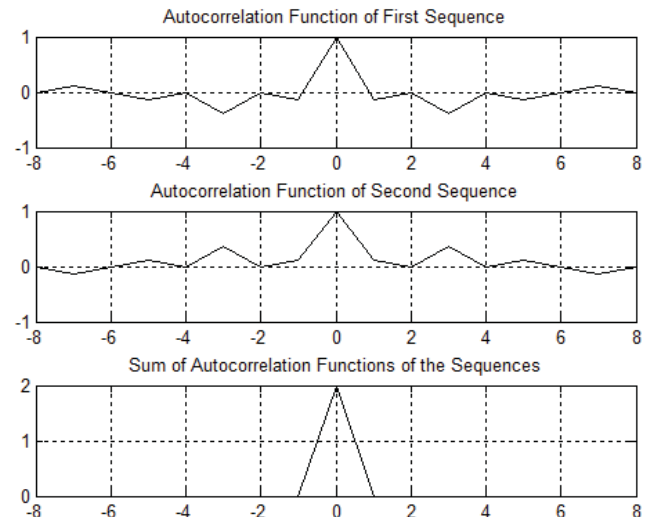
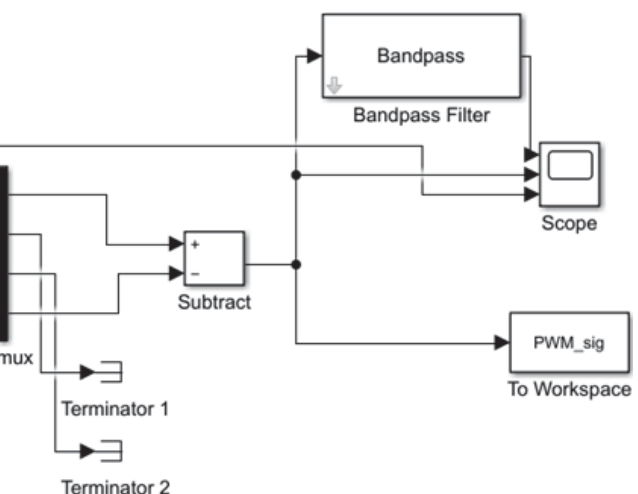


Fig. 3 Aperiodic Autocorrelations and Complementarity Condition



5. The pressure field at a point is calculated by superposing of the individual pressure generated by each small element at that point [14].

SNR improvement for the complementary Golay coded signals is calculated by,

$$SNR_{improvement}(r) = 20 \log_{10} \left(\frac{P_r}{P_{max}} \right) \quad (9)$$

where pulse excitation is used as a reference signal, $SNR_{improvement}(r)$ and P_r represent the SNR improvement and

pressure of Golay coded signal based on depth respectively. P_{max} is the maximum pressure achieved at the focal point of the transducer in case of sinusoidal burst excitation.

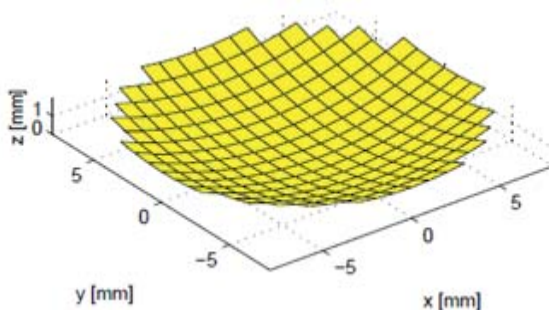


Fig. 5 Geometry of the transducer used in the simulations

B. Simulation Results

This section presents the SNR improvement of Golay coded signal with 40 chips and 2 cycles/chip compared to sinusoidal burst signal with 80 cycles. The time duration of both signals is $20\mu s$ and the excitation voltages of both signals have been adjusted to get the same spatial peak time average intensity, $I_{spta} = 0.720 W/m^2$, at the focal point.

In the first set of results shown in Fig. 6, neither attenuation nor randomly positioned scatterers exist in the medium. It seems that the Golay coded signal has improved SNR compared to the pulse excitation. Beyond 15 cm depth, SNR improvement of the Golay coded signal is depth independent and is about 7 dB at a depth of 25 cm.

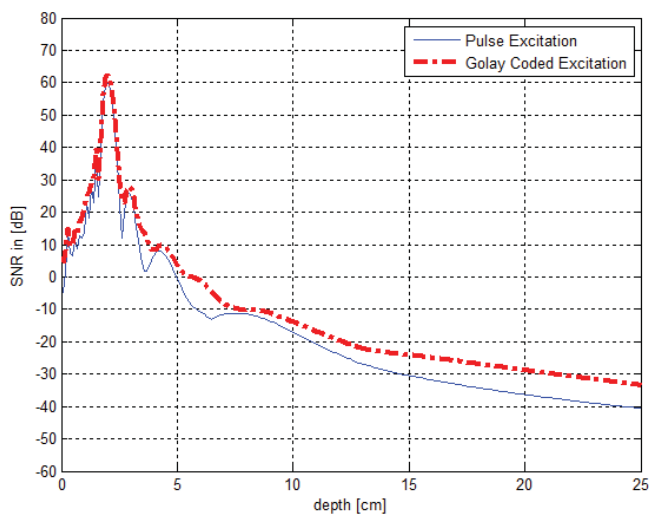


Fig. 6 Simulation results on the SNR for sinusoidal burst and a Golay coded signal. Neither attenuation nor randomly positioned scatterers exist in the simulated medium

Simulation result on the SNR improvement of the Golay coded signal in the presence of attenuation and absence of randomly positioned scatterers is shown in Fig. 7. The medium with a frequency dependent attenuation of $0.5 dB/[MHz \times cm]$ is modeled. The Golay coded signal has improved SNR compared to the pulse excitation also in the attenuating medium

[15]. Beyond 10 cm depth, SNR improvement is depth dependent due to the attenuation and improves as the depth increases. The SNR improvement of the Golay coded signal is about 14.8 dB at a depth of 25 cm while 4 dB at a depth of 10 cm.

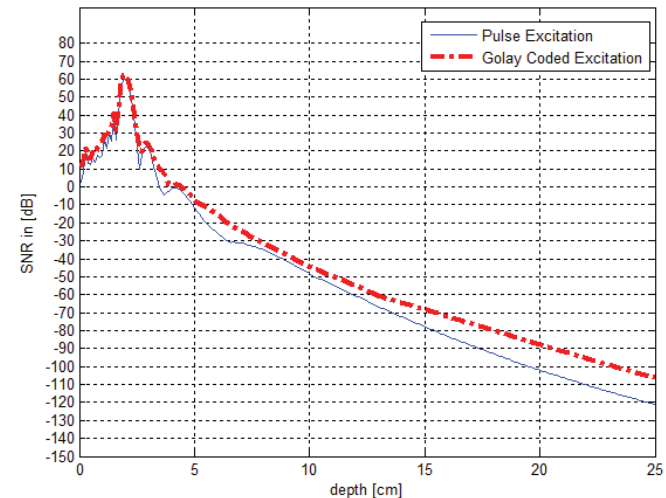


Fig. 7 Simulation results on the SNR for sinusoidal burst and a Golay coded signal under presence of attenuation and absence of randomly positioned scatterers in the simulated medium

The effects of applying matched filtering on SNR improvement is also investigated. SNR improvement for Golay coded signal in case of matched filtering increases with depth such as 8.5 dB, 13 dB, 16 dB and 17 dB at 10 cm, 15 cm, 20 cm and 25 cm depths respectively, which is shown in Fig. 8.

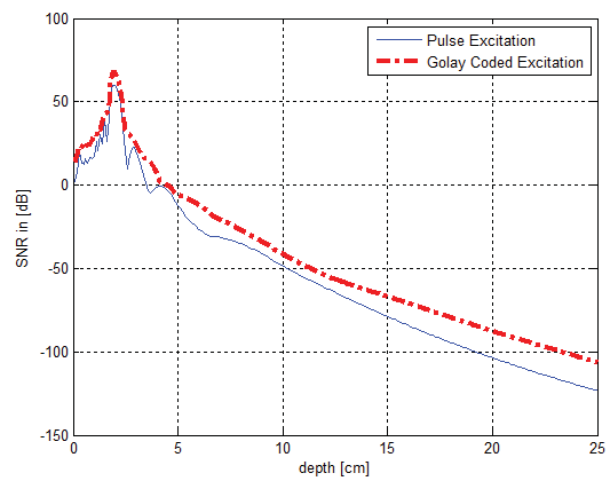


Fig. 8 Simulation results on the SNR for sinusoidal burst and a Golay coded signal under presence of attenuation and absence of randomly positioned scatterers. Matched filtering is applied

The effects of scatterers existing in the simulated medium on the received pressure signal can be destructive and the received pressure signal can be much more distorted. To investigate the effects of scatterers, breast tissue with a large number of scatterers is modeled in Field II. The density of the scatterers are chosen as $0.67 \text{ scatterers/mm}^3$. The amplitudes of

scatterers are generated according to a Gaussian distribution and scatterers are positioned according to a uniform distribution. The received pressure is calculated by superposition of all individual pressure signals received from the target and the scatterers existing in the medium [14].

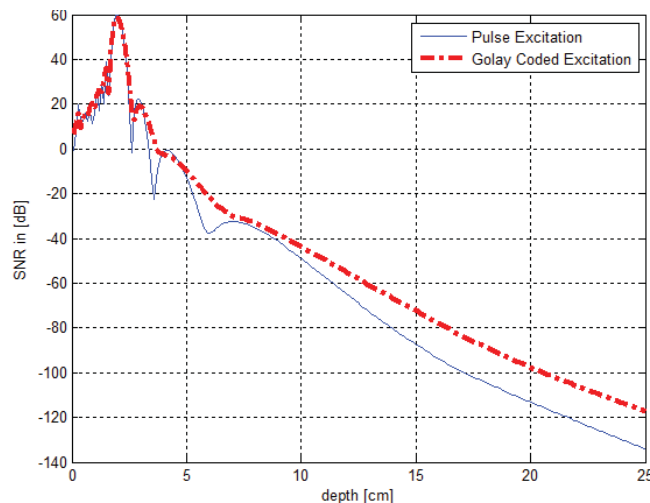


Fig. 9 Simulation results on the SNR for sinusoidal burst and a Golay coded signal under presence of attenuation and randomly positioned scatterers. Matched filtering is also applied

Fig. 9 shows that SNR improvement of Golay coded signal increases linearly with depth higher than 10 cm. Moreover, Golay coded signal has a better performance in terms of SNR improvement compared to sinusoidal burst also in a medium with a large number of scatterers.

V. EXPERIMENTAL RESULTS

A. Experimental Setup and Firing Scheme

The measurements are conducted using an experimental ultrasound research scanner, DiPhAS having 256 channels, and a phased array transducer (manufactured by company Vermon) with 7.5 MHz center frequency. DiPhAS is integrated with a multiplexer and a PC. DiPhAS enables to monitor and access to raw data at all channels and store for further digital processing. The experimental setup and the components of DiPhAS are shown in Fig. 10.

In the experiments, two Golay coded signals with 8 chips, 2 cycles/chip, and sinusoidal burst signal with 16 cycles are used. The time duration of both signals is 2.5 μ s. Only 64th element is fired for transmission, while all other elements are passive in transmission mode. For reception mode, all elements are used as shown in Fig 11. The received echo coming from all directions is used to construct an entire image. This firing scheme is referred to as synthetic transmit aperture imaging with a single emission [19].

B. Reference Signal Generation

An iron plate, a highly reflecting material, is used as a reflector and immersed into a water tank at approximately 4 cm depth. The sinusoidal burst, Golay coded sequence A and Golay coded sequence B are transmitted respectively and the received echoes are recorded. The received echoes at 64th channel in response to different excitation signals are shown in Fig. 12.

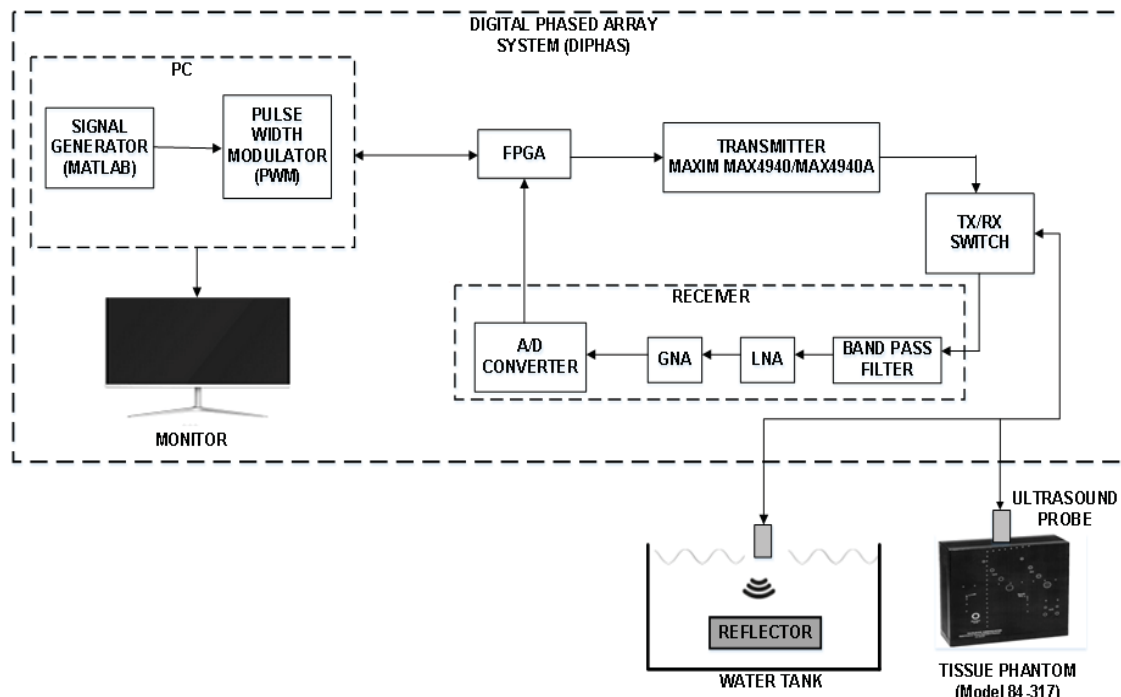


Fig. 10 The experimental setup. The components of the experimental ultrasound research scanner, DiPhAS, are shown in dashed box

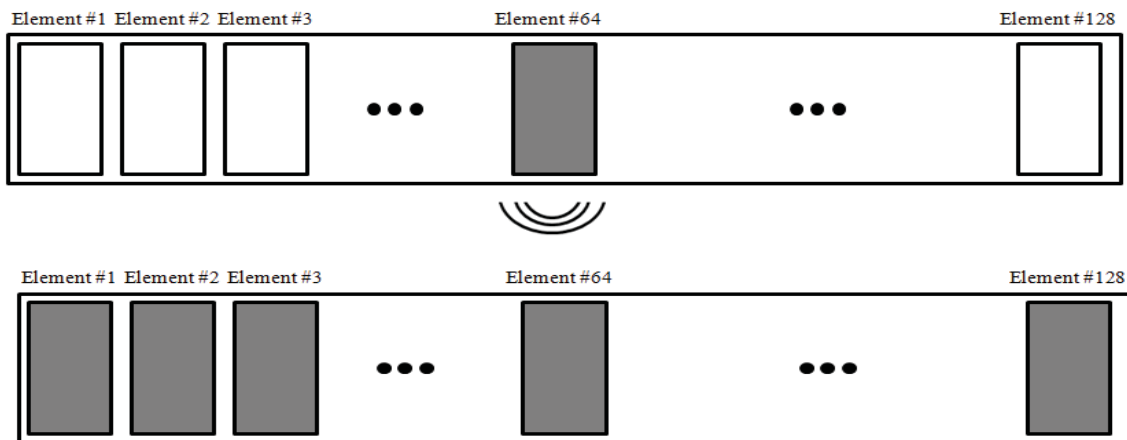


Fig. 11 Illustration of the firing scheme

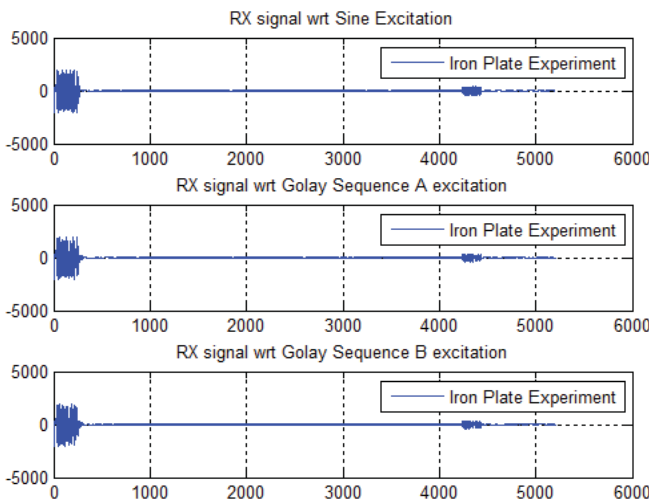


Fig. 12 The received echoes coming from the iron plate with respect to different excitation signals at 64th channel

The received echoes are converted into a unit energy signal, which is hereafter used as a reference signal in correlation calculations. Let $y_{iron}(t)$ be the received echo corresponding to a specific excitation signal. The reference signal can be denoted as:

$$x_r(t) = \frac{y_{iron}(t)}{\sqrt{\int_{-\infty}^{+\infty} y_{iron}(\tau) y_{iron}(t+\tau) d\tau}} \quad (10)$$

C. Phantom Experiments

In addition, to investigate the superiority of Golay coded signals in terms of resolution, the multipurpose tissue equivalent phantom (Model 84-317) containing a series of monofilament nylon targets (wires), 240 μm in diameter, positioned every 2 cm axially, with attenuation of 0.5 dB/[MHz \times cm] is used in the experiments. The schematic diagram of this phantom is shown in Fig. 13 (a). The scanned region of the phantom is encircled in dashed rectangular box as in Fig. 13 (b).

The experiments are repeated for the horizontal wires for different excitation signals and the received echoes are recorded. To obtain the images, the geometry provided in

Fig. 14 is used. The array is assumed to be positioned on x axis and the z axis represents the depth. Approximately 100000 points are generated in the entire region each of which is separated $\lambda/2$ in both lateral and axial direction. The area consisting of approximately 12000 points shown in rectangular dashed box is the region of interest. Applying correlation-based beamforming on the stored data provides the intensities of each point in the region of interest and the intensity, I , for each point can be expressed as:

$$z_i(t) = x_r(t) \otimes y_i(t)$$

$$c_{p,i} = z_i(t) \text{ calculated @ } N$$

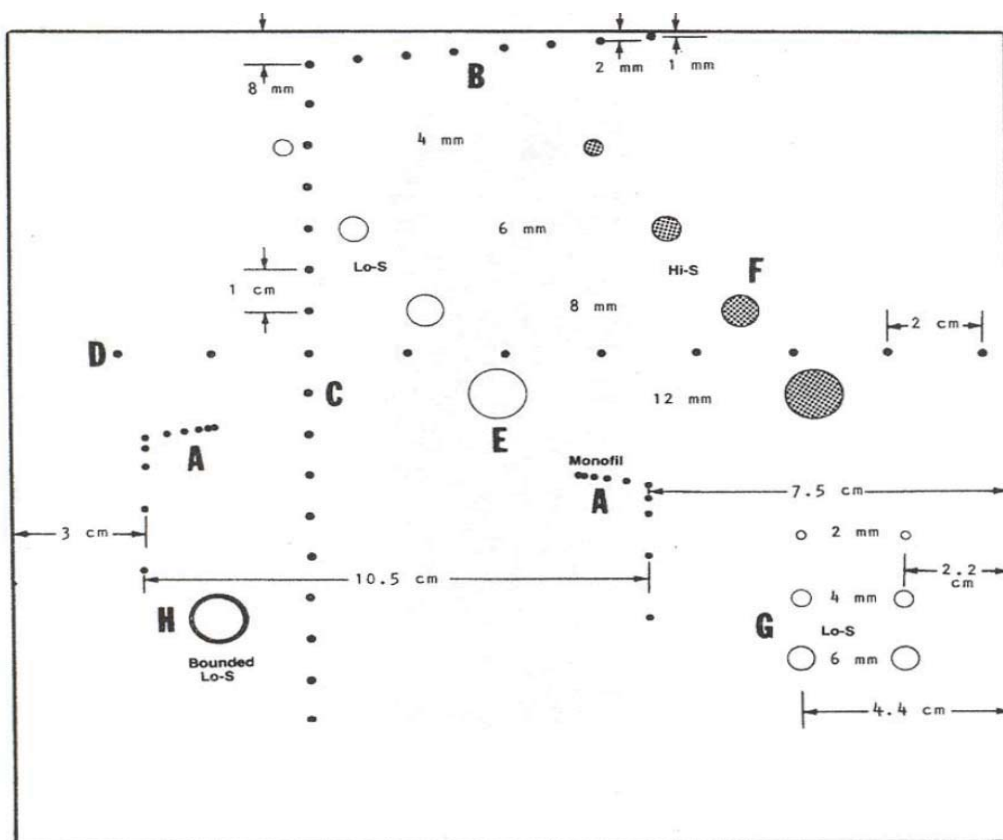
$$N = \left(\frac{d_{64,p} + d_{p,i}}{c_0} \right) / \left(\frac{1}{f_s} \right) \quad (11)$$

$$I_p = \left| \sum_{i=1}^{128} c_{p,i} \right|$$

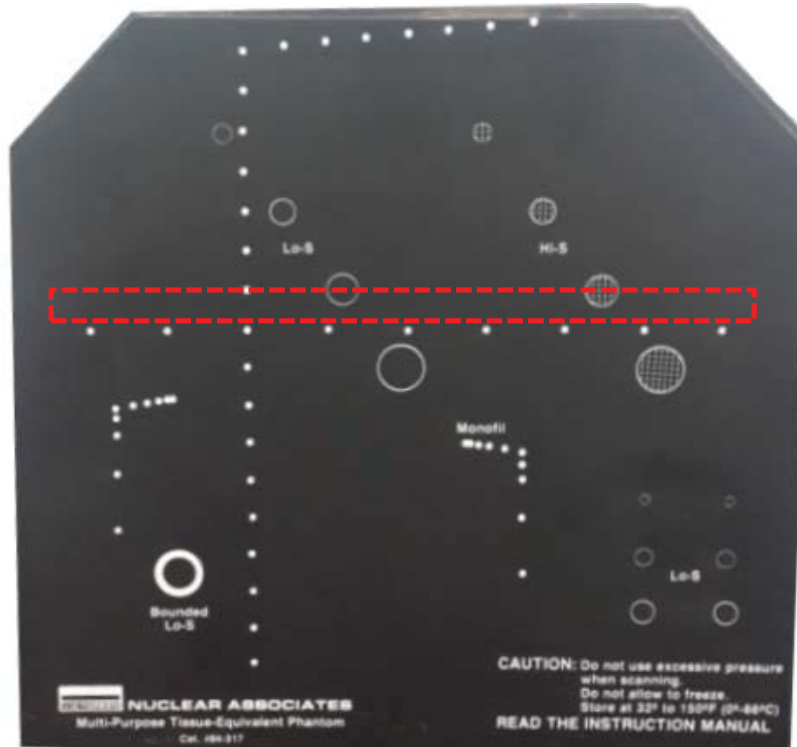
where c_0 is the speed of sound in the medium, f_s is the sampling frequency in reception mode, $d_{64,p}$ is the distance from the transmission element (64th element) to the point p , $d_{p,i}$ is the distance from point p to the element i , $z_i(t)$ is the correlation between the reference signal $x_r(t)$ and the received signal at element i , $c_{p,i}$ is the contribution of point p into $z_i(t)$ and I_p is the intensity of point p .

Once the intensity of each point is found, the images corresponding to sinusoidal burst and complementary Golay coded signals are constructed and shown in Fig. 15. In the pulsed image of Fig. 15 (a), the horizontal wire positioned at 2 cm cannot be resolved; however, the wire is resolvable in the Golay coded images of Figs. 15 (b) and (c).

Due to the complementary property of Golay sequences, combining the two coded images produces a high-resolution image which is depicted in Fig. 15 (d). It can be obtained in Fig. 15 (d) that when the complementary Golay sequences are combined coherently, significant sidelobe cancellation is achieved. Thus, it can be stated that complementary Golay sequences provide an image with better quality compared to sinusoidal burst in an attenuating medium [16]-[18].



(a)



(b)

Fig. 13 (a) Schematic diagram of the multipurpose tissue equivalent phantom (Nuclear Associates Model 84-317, Fluke Biomedical) under examination; (b) The photography of the tissue phantom. The scanned area is marked with a dashed rectangle (the characters on the phantom is not legible)

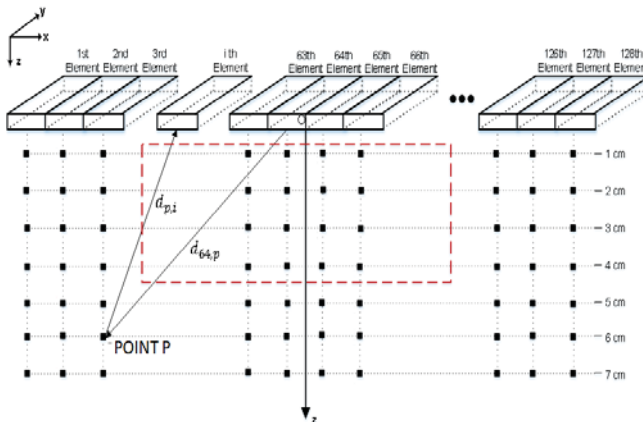


Fig. 14 Representation of the region of interest marked by a rectangle. Each point represents a pixel in the image

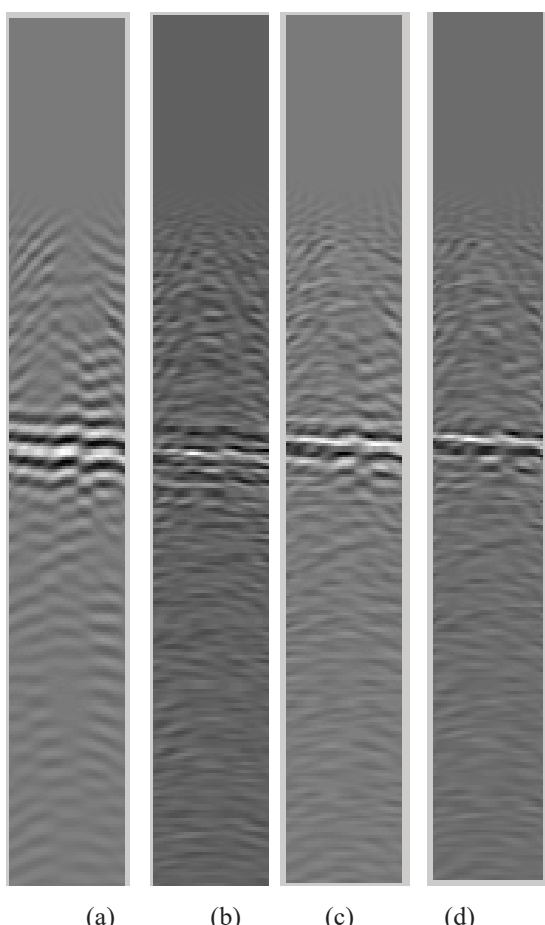


Fig. 15 Images for (a) sinusoidal burst excitation (b) Golay Sequence A excitation (c) Golay Sequence B excitation (d) Combined Golay Sequences

D. Evaluation of Image Contrast

In this section, image contrast is investigated which is defined as the ratio between the maximum intensity in the image, I_{max} , and the rms intensity of the image background, I_{rms} . Image background is the region where a target does not exist. Image contrast in linear scale can be expressed as:

$$c_r = \frac{I_{max}}{I_{rms}} \quad (12)$$

where c_r is the image contrast in linear scale. The image contrast is calculated as 2.1 for sinusoidal burst signal, 2.6 for Golay sequence A, 2.11 for Golay sequence B and 2.4 for combined Golay sequences.

VI. CONCLUSIONS AND DISCUSSIONS

The main aim of our study is to detect breast microcalcifications of $50 \mu\text{m}$ size under very weak signal conditions by using complementary Golay coded sequences. Firstly, this paper describes some fundamental concepts such as matched filtering, beamforming and PWM. A method of generating the pairs of complementary Golay sequences is also provided. Moreover, SNR improvement as a function of depth for Golay coded signals both in the absence and the presence of attenuation and the scatterers is demonstrated. Simulation results show that a substantial SNR improvement is obtained by using Golay coded signals compared to sinusoidal burst. For example, SNR improvement of 8.5 dB, 13 dB, 16 dB and 17 dB for Golay coded signal at 10 cm, 15 cm, 20 cm and 25 cm depths respectively is obtained compared to the sinusoidal burst in the presence of attenuation and matched filtering. Experimental results also show that the improvement in SNR and overall range resolution is evident when Golay coded signals are used. The energy within the code sidelobe regions is significantly reduced by using complementary Golay sequences, due to their complementarity property.

In addition, we will also use Multi-Modality Breast Biopsy and Sonographic Trainer Phantom (Model 073, CIRS) having microcalcifications of $100-300 \mu\text{m}$ embedded within the breast background by employing different firing schemes, transmission and reception parameters for further assessments as a future work.

ACKNOWLEDGMENT

The authors would like to thank Dr. S. Güler for help with the software support and S.Tasdelen for valuable discussions, the acoustic group of Bilkent University for their contribution to improve this work and reviewers for their excellent comments.

REFERENCES

- [1] Yasin KUMRU, "Using Spread Spectrum Coded Pings in Active Sonar Technology", Bilkent University, M.Sc. Thesis, July 2014.
- [2] M.O.Gülcüyüz, "Low Power Range Estimation with DSSS technique In Underwater Acoustics", Bilkent University, M.Sc. Thesis, August 2013.
- [3] Pearson, Medical Imaging Signals and Systems, Prince & Links, 2/2014.
- [4] U.Madhow, Fundamentals of Digital Communication, Cambridge Universty Press 2008.
- [5] C.A.Balanis, Antenna Theory, Wiles Interscience, Third Edition,2005.
- [6] D.T.Blackstock, Fundamentals of Physical Acoustics.
- [7] W.S.Burdic, Underwater Acoustic System Analysis.Prentice Hall,1984.
- [8] R.J.Urick, Principles of Underwater Sound. Peninsula Publishing 3rd edition,1983.
- [9] M.J.E.Golay, "Complementary Series", IRE Transactions on Information Theory, vol IT-7, pp 82-87, 1961.
- [10] D.Z.Dokovic,"Equivalence Classes and Representatives of Golay Sequences" Discrete Mathematics 189 (1998) 79-93.
- [11] Elena Kalashnikov, "An Introduction to Golay Complementary

- Sequences”, Department of Mathematics, University of Alberta, 2004.
- [12] S.Kounias, C.Koukouvinos and K.Sotirakoglou “On Golay Sequences” Discrete Mathematics 92 (1991) 177-185, 1988.
 - [13] I.Trots, A.Nowicki, W.Secomski, J.Litniewski “Golay Sequences-Side Lobe-Canceling Codes For Ultrasonography”, Archives of Acoustics, 2004.
 - [14] J.A.Jensen, “Field: A Program for simulating ultrasound systems”.
 - [15] T.X.Misaridis and J.A JENSEN, “Use of Modulated Excitation Signals in Medical Ultrasound. Part I: Basic concepts and Expected Results”, IEEE Transactions on Ultrasonics, Ferroelectrics and Frequency Control, Vol.52, No.2, February 2005.
 - [16] T.X.Misaridis and J.A JENSEN, “Use of Modulated Excitation Signals in Medical Ultrasound. Part II: Design and Performance for Medical Imaging Applications”, IEEE Transactions on Ultrasonics, Ferroelectrics and Frequency Control, Vol.52, No.2, February 2005.
 - [17] T.X.Misaridis and J.A JENSEN, “Use of Modulated Excitation Signals in Medical Ultrasound. Part III: High Frame Rate Imaging”, IEEE Transactions on Ultrasonics, Ferroelectrics and Frequency Control, Vol.52, No.2, February 2005.
 - [18] R.Y.Chiao and X.Hao, “Coded Excitation for Diagnostic Ultrasound: A System Developer’s Perspective”, IEEE Transactions on Ultrasonics, Ferroelectrics and Frequency Control, Vol.52, No.2, February 2005.
 - [19] I.Trots, Y.Tasinkevych, A.Nowicki, M.Lewandowski, “Coded Transmission in Synthetic Transmit Aperture Ultrasound Imaging Method”, WASET, 2012.
 - [20] J.f.Synnevag, S.Holm, “Adaptive Beamforming Applied to Medical Ultrasound Imaging”, IEEE Transactions on Ultrasonics, Ferroelectrics and Frequency Control, August 2007.
 - [21] L.Huang, Y.Labyed, F.Simonetti, M.Williamson, R.Rosenberg, P.Heintz, D.Sandoval, “High-resolution imaging with a real-time synthetic aperture ultrasound system: A phantom study”, 2011 SPIE Medical Imaging Meeting.
 - [22] M.Lewandowski, A.Nowicki, “Universal Coded Ultrasound Imaging System with Software Processing”, Archives of Acoustics, 32, 4 (Supplement), 81-86 (2007).
 - [23] B.Haider, P.A.Lewin, K.E.Thomenius, “Pulse Elongation and deconvolution filtering for medical ultrasound imaging”, IEEE Transactions on UFSC, Volume:45, Issue:1, Jan.1998.